

Population pharmacokinetics of tanezumab in phase 3 clinical trials for osteoarthritis pain

E. Niclas Jonsson,¹ Rujia Xie,² Scott F. Marshall³
& Rosalin H. Arends⁴

¹Pharmetheus AB, Uppsala, Sweden, ²Pfizer Ltd., Shanghai, China, ³Pfizer Ltd., Sandwich, UK and ⁴Pfizer Inc, Groton, CT, USA

WHAT IS ALREADY KNOWN ABOUT THIS SUBJECT

- Tanezumab is an IgG2 that binds nerve growth factor and represents a novel treatment for chronic pain. Published pharmacokinetic (PK) data from a phase 2 study in the treatment of patients with OA indicated body weight was an important covariate.

WHAT THIS STUDY ADDS

- The results add to our knowledge of which clinical covariates should be considered to explain inter-individual variability of exposure to therapeutic antibodies. Comparative analysis of dosing strategies supports use of a fixed-dosing approach for further development.
- This work presents the most complete understanding of tanezumab PK to date and answers a key question on the risk : benefit of tanezumab by illustrating that exposure of tanezumab is not significantly altered by identified covariates to an extent that would require dose adjustment.

AIMS

The aims were to 1) develop the pharmacokinetics model to describe and predict observed tanezumab concentrations over time, 2) test possible covariate parameter relationships that could influence clearance and distribution and 3) assess the impact of fixed dosing vs. a dosing regimen adjusted by body weight.

METHODS

Individual concentration–time data were determined from 1608 patients in four phase 3 studies conducted to assess efficacy and safety of intravenous tanezumab. Patients received two or three intravenous doses (2.5, 5 or 10 mg) every 8 weeks. Blood samples for assessment of tanezumab PK were collected at baseline, 1 h post-dose and at weeks 4, 8, 16 and 24 (or early termination) in all studies. Blood samples were collected at week 32 in two studies. Plasma samples were analyzed using a sensitive, specific, validated enzyme-linked immunosorbent assay.

RESULTS

A two compartment model with parallel linear and non-linear elimination processes adequately described the data. Population estimates for clearance (CL), central volume (V_1), peripheral volume (V_2), inter-compartmental clearance, maximum elimination capacity (VM) and concentration at half-maximum elimination capacity were 0.135 l day⁻¹, 2.71 l, 1.98 l, 0.371 l day⁻¹, 8.03 µg day⁻¹ and 27.7 ng ml⁻¹, respectively. Inter-individual variability (IIV) was included on CL, V_1 , V_2 and VM. A mixture model accounted for the distribution of residual error. While gender, dose and creatinine clearance were significant covariates, only body weight as a covariate of CL, V_1 and V_2 significantly reduced IIV.

CONCLUSIONS

The small increase in variability associated with fixed dosing is consistent with other monoclonal antibodies and does not change risk : benefit.

Correspondence

Dr. Rosalin H. Arends, Pharmetheus AB, 445 Eastern Point Road, Groton, CT 06340 USA
Tel.: +86 0326 1547
E-mail: Rosalin.arends@pfizer.com

Keywords

population pharmacokinetics, tanezumab

Received

22 June 2015

Accepted

23 November 2015

Accepted Article Published Online

27 November 2015

Introduction

At least 116 million adults in the United States are burdened by chronic pain at some point in their lives, leading to an annual cost of \$560–\$635 billion for direct medical treatment and lost productivity [1]. Although paracetamol (acetaminophen), non-steroidal anti-inflammatory drugs (NSAIDs) and opioids are considered the gold standard analgesic drugs in clinical practice [2], management of chronic pain is often ineffective or incomplete. Therefore, effective pain relief represents an unmet medical need [3, 4]. The cardiovascular risks and gastrointestinal, hepatic and renal side effects of NSAIDs and paracetamol may limit the use of these medications [4, 5]. Similarly, opioids are associated with a broad spectrum of side effects as well as the potential for loss of effectiveness, constipation, drug diversion or addiction, respiratory depression and accidental death from overdose [2, 4].

Nerve growth factor (NGF) is a mediator of biological mechanisms that cause pain [6]. Elevated NGF levels are associated with inflammation, tissue damage and diseases such as arthritis. NGF administration causes pain, whereas blockade of NGF activity reduces pain [3]. As a result, targeting NGF is a new mechanism being investigated for the treatment of moderate to severe chronic pain. Tanezumab is a humanized immunoglobulin G (IgG) 2 monoclonal antibody that binds to NGF with high affinity and specificity and effectively blocks NGF activity [7]. Tanezumab or its murine precursor is an effective analgesic in animal models of pathological pain, including arthritis and cancer pain [8, 9]. In randomized clinical trials in patients with osteoarthritis (OA) and chronic low back pain, tanezumab has demonstrated consistent efficacy across the domains of pain and physical function [10–12].

An initial population model describing the pharmacokinetics (PK) and pharmacodynamics (PD) of a wide dose range of tanezumab in patients with OA was used to determine the dose and dose regimen for further development [13, 14]. The current analysis characterizes PK across four randomized double-blind placebo-controlled phase 3 clinical trials conducted to assess efficacy and safety of intravenous (i.v.) tanezumab in patients with moderate to severe pain due to OA. The aim was to 1) develop further the PK model to describe and predict observed tanezumab concentrations over time, 2) test possible covariate parameter relationships (i.e. demographics and/or disease characteristics) that could influence clearance and distribution and 3) assess the impact of fixed dosing vs. a dosing regimen adjusted by body weight (WT).

Methods

Study site and ethical approval

Plasma tanezumab concentration–time data were collected during four randomized, double-blind, placebo-controlled,

multicentre, parallel group phase 3 studies of tanezumab in patients with moderate to severe OA of the knee or hip [10, 11, 15]. Studies were registered (ClinicalTrials.gov identifiers: NCT00733902 [A4091011], NCT00744471 [A4091014], NCT00830063 [A4091015] and NCT00863304 [A4091018]) and were conducted in compliance with the Declaration of Helsinki and the International Conference on Harmonization Good Clinical Practice guidelines. Protocols were reviewed and approved by an institutional review board at each study site. Written informed consent was obtained from each patient before initiation of protocol-specified procedures.

Treatment and sample collection

Each patient was administered tanezumab 2.5 mg, tanezumab 5 mg, tanezumab 10 mg or placebo every 8 weeks for a total of two (studies A4091015 and A4091018) or three (studies A4091011 and A4091014) doses via i.v. infusion over a 5 min period. Blood samples for assessment of tanezumab PK were collected at baseline (pre-dose), 1 h post-dose and at weeks 4, 8 (pre-dose and post-dose), 16 (pre-dose and post-dose) and 24 (or early termination) in all studies. Blood samples were also collected at week 32 in studies A4091011 and A4091014.

Bioanalytical PK assay

Plasma samples were analyzed using a sensitive, specific, validated enzyme-linked immunosorbent assay for tanezumab with a lower limit of quantification (LLOQ) of 12.0 ng ml⁻¹ and with a range of 12 to 384 ng ml⁻¹ in 100% human plasma (see Supporting Information). Results were analyzed via four parameter logistic curve-fitting programmes and 1/y² weighting (Gen5 Secure Software version 1.02 or higher, Winooski, VT, USA). In each of seven analysis runs (performed over 3 days), three replicates of quality control (QC) samples at five concentrations (12.0, 30.0, 150, 300 and 384 ng ml⁻¹) were analyzed. Precision, defined by the coefficient of variation (standard deviation/mean × 100), was determined from interpolated (observed) QC sample concentrations and ranged from 2.08% to 11.5% for the inter-runs and ranged from 0.337% to 11.8% for the seven intra-runs. Accuracy was defined by the percent relative error ($[(\text{observed concentration}/\text{nominal concentration}) - 1] \times 100$), and ranged from 0.833% to 7.33% for the inter-runs and from 0% to 15.3% for the intra-runs. To evaluate dilution linearity, six different dilutions were assessed: minimum dilution (1 : 20), 1 : 2000, 1 : 4000, 1 : 6667, 1 : 13 333 and 1 : 133 333. The acceptance criteria were met up to the 13 333-fold dilution with the samples diluted 6667-fold and 13 333-fold showing precision of 0.654% and 1.25%, respectively, and accuracy of 6.00% and 10.7%, respectively, indicating that this assay can accurately measure free tanezumab concentration up to 5 mg ml⁻¹.

Final analysis data set

During assembly of the PK data set that was compatible with the modelling software (NONMEM, ICON Development Solutions, Hanover, MD, USA), a number of data issues were identified (for example, unrealistic peak : trough ratios) that were judged likely to have a significant impact on the model building process and covariate identification. To handle the most likely incorrect data which probably originated from either not matching the correct sample with the correct prelabelled collection tube or collecting both pre- and post-dose samples either pre-dose or post-dose, the following cleaning rules were applied:

- 1) Individuals ($n = 4$) with baseline PK observation $\geq 750 \text{ ng ml}^{-1}$ and a sample after the first dose in the range of 40–384 ng ml^{-1} were excluded. The range of 40–384 ng ml^{-1} was used for the apparent post-sample because this was the range of matrix interference in baseline samples. The cut off value for the apparent baseline sample was set at 750 ng ml^{-1} since it was two-fold above the maximum baseline background interference and represented 80% of the post first dose 2.5 mg C_{max} .
- 2) Each pair of peak/trough observations in which the ratio was < 2 was excluded ($n = 188$). This exclusion rule addressed specific pre-dose/post-dose (peak/trough) sample pairs that were close in value which could happen if, in error, the post-dose sample was collected pre-dose, or the pre-dose sample collected post-dose. A ratio < 2 was selected for the cut-off value since this is an unrealistic value considering the expected peak : trough ratio was 10 : 1 based on phase 1 data.
- 3) The complete PK profile of patients who still had baseline observations ≥ 0 was excluded ($n = 190$). This exclusion criterion was necessary since there were still subjects with detectable levels of drug in the baseline samples despite rules one and two due to lack of a first post-dose sample to help interpret baseline values.

Finally, outlying data points were identified based on initial modelling results and distribution of conditional weighted residuals (CWRES). Data points associated with absolute CWRES > 5 were regarded as outliers and were excluded from further model development. These outlying data points as well as patients excluded based on cleaning rule 3 ($n = 190$) were re-included when the final model was established to assess their impact on parameter estimates.

Pharmacokinetic analysis

All analyses were performed in accordance with appropriate regulatory guidelines [16, 17]. NONMEM version 7.1

was used with Fortran compiler IntelR64 Fortran Professional Compiler version 11.1. The first order conditional estimation method (with or without INTERACTION as appropriate) was used for all analyses. The final model was implemented in ADVAN6. Automated NONMEM run procedures, such as the stepwise covariate model (SCM) building procedure in Perl-speaks-NONMEM (PsN) and visual predictive check (VPC), were implemented using PsN version 3.2.4 [18]. Results were further processed using R Software version 2.10.1. Xpose version 4 was used as an aid in model assessment [19].

Previous work based on phase 1 and 2 data indicated that a two compartment model described tanezumab PK adequately over the clinical dose range. In this two compartment model, WT was an important predictor for interindividual variability in clearance (CL), central volume of distribution (V_1) and peripheral volume of distribution (V_2). Inter-individual variability (IIV) was included on CL, V_1 and V_2 assuming an exponential distribution and variability in residual error was accounted for by log transformation of both sides (i.e. approximately constant coefficient of variation model). This model was used as a starting point for the development of the base PK model for the phase 3 data. Because WT was important in the previous model, different body size measures (WT, body surface area [BSA], body mass index [BMI] and baseline lean body weight [BLBW]) were considered as structural covariates in the form of power functions in the base PK model for the phase 3 data. In addition to body size as a structural covariate, different structural PK models (one and three compartment models, with and without non-linear elimination) were also considered, as well as other IIV and residual error structures. Variability estimates were reported as the coefficient of variation (%CV, calculated as the square root of variance) estimated by assuming the exponential distribution (IIV) or under the log transformation (residual error).

The appropriateness of the base PK model was assessed by inspection of residual plots and visual predictive checks (VPCs). This basic PK model with the supported IIV terms was used as the starting point for covariate model development. Various patient/disease characteristics were evaluated, including dose, age, gender and race on CL, V_1 and V_2 and race, gender and age on maximum elimination capacity (VM) and concentration at half-maximum elimination capacity (KM). In addition, creatinine clearance (CL_{cr}) was tested on CL and was computed using the Cockcroft–Gault formula utilizing total body weight [20]. Since this formula leads to unreasonably high values for heavy subjects [21], CL_{cr} values were truncated at a maximum value of 150 ml min^{-1} . Also, the impact of OA joint (knee or hip) was investigated on all structural model parameters. Missing values for covariates were imputed with the median value or common category during analysis (with

the exception that missing values for OA joint were imputed as knee because missing values occurred only in study A4091011, which only enrolled patients with knee OA). Only a few cases of patients were reported with samples that were positive for anti-drug antibodies (8/1601 patients). Since the PK, clinical pain relief response and safety profile were not different in ADA-positive subjects compared with ADA-negative subjects, ADA status was not included as a variable in the covariate model building.

Covariate model building was performed using the SCM procedure in PsN [18]. The covariate search was not done in one forward and one backward step as is the default in SCM. Instead, to manage the time to complete each run, an initial univariate step was performed to identify the most relevant covariates, followed by two forward/backward searches. More specifically, the search was done as 1) test all parameter-covariate relations on a univariate basis and retain only those covariates that were significant at the $P < 0.05$ level, 2) perform a full forward/backward search with covariates retained from step one with significance levels set to $P < 0.01$ and $P < 0.001$ for the forward and backward step, respectively, and 3) perform a second search with the final model from step two and those covariates excluded from step one with significance levels set to $P < 0.01$ and $P < 0.001$ for the forward and backward step, respectively. Continuous covariate relationships were coded as power models and categorical covariates were coded as a fractional difference to the common category (Equation 1). Reported confidence intervals were computed from the standard error estimates obtained from NONMEM.

$$\text{ParCov}_j = (\text{Cov}_j / \text{Cov}_{i,\text{median}})^{\theta_j}$$

$$\text{ParCov}_j = 1 \text{ if most common category or } 1 + \theta_j \text{ if other category} \quad (1)$$

The parameter for the corresponding typical parameter for the median Cov_i and/or common category is multiplied by ParCov_j .

Performance of the final population PK model was evaluated using goodness-of-fit plots, individual plots and diagnostic plots related to the covariate and stochastic models. Predictive performance of the model was assessed through a VPC (with prediction correction), which compares the prediction interval of observed data with simulated data using the final population model [22].

The impact of fixed vs. WT-adjusted dosing was performed by simulating the PK profile for the first dosing interval for each patient, assuming either fixed dosing of 2.5, 5 or 10 mg, or WT-adjusted dosing of $\text{WT}^*[(2.5, 5 \text{ or } 10)/\text{median WT}]$ mg. The exposure range (defined as the 5th to 95th percentile) from fixed dosing was compared with predicted exposures from WT-adjusted dosing and the exposure range for WT-adjusted regimen was compared with the predicted fixed dosing.

Results

After applying all predefined rules, the final analysis data set included 1610 patients with at least one post-dose observation above the LLOQ. After removal of outliers, this number decreased to 1608 patients and 7592 observations (Table 1). Baseline demographics used for evaluating categorical covariates were similar across groups and across the four studies (Table 1).

The base PK model was a two compartment model with parallel linear and non-linear elimination with IIV on CL, V_1 , V_2 , and VM. A correlation term between IIV in CL and V_1 was also included in the model. The mean (%CV) estimates from the base model were $\text{CL} = 0.135 \text{ l day}^{-1}$ (35%), $V_1 = 2.89 \text{ l}$ (27%), $V_2 = 1.81 \text{ l}$ (20%) and $\text{VM} = 10 \mu\text{g day}^{-1}$ (37%).

The addition of non-linear PK by including a Michaelis–Menten (MM) component (leading to a decrease in objective function value [Δ OFV] of 359 points) helped account for trends in CWRES vs. predicted concentration and in CWRES vs. time plots. Graphical analysis plots (not shown) demonstrated that a less heavily-tailed distribution of the residual error could be obtained via addition of a second residual error term through a mixture model (Equation 2). The estimate for the mixture probability for the smaller residual error term in the final model was 0.76 and the residual variabilities were estimated to be 13% and 54% for the higher and lower probability, respectively (Table 2).

$$Y_{ij} = \hat{Y}_{ij} + \varepsilon_1 \text{ if subpopulation 1 or } \varepsilon_2 \text{ if subpopulation 2.} \quad (2)$$

where Y_{ij} is the i th individual's j th observation and \hat{Y}_{ij} is the corresponding model prediction.

WT, BSA, BMI and BLBW were tested on CL, V_1 and V_2 to determine the best measure of body size. Inclusion of WT resulted in the largest Δ OFV when added as a covariate on CL. Whereas BLBW resulted in the largest Δ OFV when included as a covariate on V_1 and V_2 , little difference was noted in fit of the models on CL, V_1 and V_2 . Therefore, WT was selected as the body size measure to include as a structural covariate in the base PK model.

Covariate model development used CL, VM, KM, V_1 and V_2 as parameters for evaluation of the covariates dose (only on CL, V_1 and V_2), age, race, gender, site of OA and CL_{cr} (only on CL). The SCM procedure in PsN resulted in a final covariate model with CL_{cr} , gender and dose (2.5 and 5 mg vs. 10 mg) on CL, and gender on V_1 in addition to WT as a structural covariate on CL, V_1 and V_2 (Equations 3–5). Gender on CL was identified as a significant covariate in the second full forward/backward search.

Table 1

Summary statistics of the continuous covariates

	Tanezumab 2.5 mg <i>n</i> = 289	Tanezumab 5 mg <i>n</i> = 655	Tanezumab 10 mg <i>n</i> = 664	All <i>n</i> = 1608
Age (years)				
Mean ± SD	61.7 ± 10.0	61.4 ± 10.5	61.2 ± 10.5	61.4 ± 10.4
Range	26–88	21–93	32–92	21–93
Weight (kg)				
Mean ± SD	86.3 ± 18.3	86.8 ± 17.7	86.6 ± 17.7	86.6 ± 17.8
Range	44.9–133	44.4–145	34–170	34–170
Creatinine clearance (ml min⁻¹)				
Mean ± SD	96.0 ± 28.7	97.1 ± 31.4	98.9 ± 32.2	97.7 ± 31.3
Range	37.7–197	30.3–301	27.5–242	27.5–301
Race, <i>n</i> (%)*				
White	253 (87.5)	575 (87.8)	561 (84.5)	1389 (86.4)
Black	30 (10.4)	72 (11.0)	78 (11.7)	180 (11.2)
Asian	3 (1.0)	4 (0.6)	8 (1.2)	15 (0.9)
Other	3 (1.0)	4 (0.6)	17 (2.6)	24 (1.5)
Gender, <i>n</i> (%)				
Female	173 (59.9)	396 (60.5)	404 (60.8)	973 (60.5)
Male	116 (40.1)	259 (39.5)	260 (39.2)	635 (39.5)
Index joint, <i>n</i> (%)				
Knee	292	656	664	1612
Hip	143 (49.0)	479 (73.0)	491 (73.9)	1113 (69.0)
Hip	149 (51.0)	177 (27.0)	173 (26.1)	499 (31.0)

*Not all percentages sum to 100.0% due to rounding.

$$CLWT_i = (WT_i/84.7)^{08}$$

$$CLCL_{Cr_i} = (CL_{Cr_i}/93.5)^{011}$$

$$CLDOSE_i = 1 \text{ if dose} = 10 \text{ mg or } 1 + \theta_{12} \text{ if dose} = 2.5 \text{ or } 5 \text{ mg} \quad (3)$$

$$CLGENDER_i = 1 \text{ if female or } 1 + \theta_{14} \text{ if male}$$

$$TVCL_i = \theta_1 \cdot CLWT_i \cdot CLCL_{Cr_i} \cdot CLDOSE_i \cdot CLGENDER_i$$

TVCL_{*i*} denotes the *i*th individual's typical value of CL, and $\theta_{8,11,12,14}$ are parameters of the model that describes the influence of the corresponding covariate. θ_1 is the CL of a hypothetical female patient weighing 84.7 kg with a CL_{Cr} of 93.5 ml min⁻¹ after a dose of 10 mg.

$$V_1WT_i = (WT_i/84.7)^{09}$$

$$V_1GENDER_i = 1 \text{ if female or } 1 + \theta_{13} \text{ if male} \quad (4)$$

$$TVV_{1i} = \theta_2 \cdot V_1WT_i \cdot V_1GENDER_i.$$

TVV_{1*i*} denotes the *i*th individual's typical value of V₁, and $\theta_{9,13}$ are parameters of the model that describe the influence of the corresponding covariate. θ_2 is the V₁ of a hypothetical female patient weighing 84.7 kg.

$$V_2WT_i = (WT_i/84.7)^{010} \quad (5)$$

$$TVV_{2i} = \theta_4 \cdot V_2WT_i$$

TVV_{2*i*} denotes the *i*th individual's typical value of V₂, and θ_{10} is a parameter of the model that describes the influence of body weight on V₂. θ_4 is the V₂ of a hypothetical patient weighing 84.7 kg.

Estimated values for the final population PK model parameters of CL, V₁, V₂ and VM for a typical female patient weighing 84.7 kg with a CL_{Cr} of 93.5 ml min⁻¹ after tanezumab 10 mg were 0.135 l day⁻¹, 2.71 l, 1.98 l and 8.03 μg day⁻¹, respectively (Table 2). Estimates of IIV (as %CV) associated with CL, V₁, V₂ and VM were 26%, 20%, 20% and 41%, respectively. The correlation between IIV of CL (η_{CL}) and V₁ (η_{V1}) was 0.67. The η shrinkages were reasonably low for CL and V₁ (11%/10% and 15%/23%, respectively, for the low/high residual error mixtures) but large for VM and V₂ (66%/71% and 57%/79%, respectively). However, the condition number was low (169) and the correlation between the parameter estimates indicated that the model is not over-parameterized.

All PK parameters were estimated with good precision, as reflected by the narrow range for 95% confidence intervals (CI, Table 2). The final model provided a good fit to the data with good agreement between observed and model predicted (using either

Table 2

The parameter estimates of the final model

Parameter	Estimate	95% CI*
CL† (l day ⁻¹)	0.135	0.129, 0.14
V ₁ † (l)	2.71	2.66, 2.76
Q† (l day ⁻¹)	0.371	0.198, 0.545
V ₂ † (l)	1.98	1.72, 2.24
Mixture probability with low RSV	0.763	0.738, 0.789
KM (ng ml ⁻¹)	27.7	7.8, 47.7
VM (µg day ⁻¹)	8.03	5.72, 10.3
WT on CL	0.77	0.682, 0.858
WT on V ₁	0.554	0.489, 0.62
WT on V ₂	0.302	0.15, 0.454
CL _{cr} on CL	0.108	0.0738, 0.141
Dose on CL	0.0669	0.0346, 0.0992
Gender on V ₁	0.175	0.143, 0.208
Gender on CL	0.143	0.106, 0.181
IIV CL, %CV	26	25, 27
IIV V ₁ , %CV	20	19, 21
Cov CL-V ₁ ‡	0.034	0.03, 0.038
IIV VM, %CV	41	26, 52
IIV V ₂ , %CV	20	15, 24
Low RSV, %CV	13	13, 13
High RSV, %CV	54	52, 55

*Confidence interval computed from the standard error estimates obtained from NONMEM. †The estimate is for a female weighing 84.7 kg with a CL_{cr} of 93.5 ml min⁻¹. ‡Estimate of the covariance between CL and V₁. CI, confidence interval; CL, clearance; CL_{cr}, creatinine clearance; Cov, covariance; %CV, coefficient of variation (calculated by taking the square root of variance estimated by NONMEM); IIV, inter-individual variability; KM, concentration at half maximum elimination capacity; Q, inter-compartmental clearance; RSV, residual variability; V₁, central volume; V₂, peripheral volume; VM, maximum elimination capacity; WT, body weight.

population [PRED] or individual [IPRED] predictions) tanezumab concentrations. Also, there were no unacceptable trends in CWRES vs. population predictions or over time to indicate that a more elaborate residual error structure was needed (Figure 1).

When the data points associated with absolute CWRES >5 (*n* = 110) and those from cleaning rule 3 (*n* = 190) were re-included in the final model, effects on the model were minimal (<10% change in most fixed parameters with a maximum change of 23% in the estimate of inter-compartmental clearance).

Predictive performance of the model was assessed through a VPC with prediction correction (Figure 2). Overall, the model predicts the observed data well since the median, 5th and 95th data percentiles were adequately captured by the corresponding simulation-based prediction intervals and 95% CI. The simulation to assess the impact of a fixed vs. WT-adjusted dosing regimen shows that fixed dose will lead to a slightly larger variability in exposure (25%–26%) compared with WT-adjusted dosing (19%–20%; Figures 2 and 3).

Discussion

Population PK of different IgG therapeutic antibodies have been widely published [23]. As is the case for tanezumab, therapeutic antibodies are commonly subject to both linear and non-linear kinetics [24]. Nonetheless, initial population PK modelling indicated a two compartment model with linear elimination adequately characterized the observed PK in phase 1 and 2 studies across a dose range of 3 to 1000 µg kg⁻¹ [13, 14]. Linear elimination of monoclonal antibodies is non-specific because it occurs via catabolism following endocytosis by the reticuloendothelial system. The process is relatively slow because the antibody can be salvaged via binding to the neonatal Fc receptor (FcRn) [25]. The half-life estimated for tanezumab in this population, 21 days [13, 26], is consistent with that of a typical IgG antibody with a long half-life (~23 days) [27]. However, the linear model used to describe the phase 2 data was inadequate for the current, larger phase 3 dataset. A better description of individual PK profiles and residual diagnostics was achieved by including a non-linear component. The similarity of the CL estimates across analyses (0.135 l day⁻¹ for the linear plus non-linear model and 0.207 l day⁻¹ for the linear model only) indicates a relatively small contribution of non-linear CL and is more important for doses <2.5 mg, whereas at doses ≥2.5 mg, the contribution of non-linear CL only accounts for 18%, 10% and 5% of total CL for 2.5, 5 and 10 mg, respectively.

The faster (0.29 l day⁻¹, VM/KM) non-linear pathway is likely related to the target binding (target-mediated drug disposition [TMDD]) which, as for other antibodies, can be adequately described by the MM equation [28, 29]. The inverse correlation of the low non-linear CL contribution to dose suggests that there is an excess of free tanezumab in the systemic circulation over the 8 week dose regimen for these doses. This is consistent with the stable therapeutic effect that has been observed at these doses in phase 3 studies.

Since NGF is a dimer [30], two tanezumab binding sites are on each molecule, at lower tanezumab concentrations a significant amount of NGF would be only half-saturated (i.e. only one of the NGF binding sites occupied, NGF monomer). CL of this NGF monomer could still occur through internalization after binding to the high affinity (tropomyosin-related kinase A, trkA) or low affinity neurotrophin (p75) receptor, which are targets for free NGF [7]. However, assuming that binding to tanezumab does not affect the NGF internalization rate, the non-linear CL associated with this monomer would most likely be faster than the 0.29 l day⁻¹ estimated for the non-linear pathway (VM/KM) and conceivably closer to values for free NGF that would have a CL of >100 l day⁻¹ in humans based on a NGF CL of 140–416 ml h⁻¹ kg⁻¹ in animals [31, 32]. Therefore, it is possible that the estimated non-linear CL could be

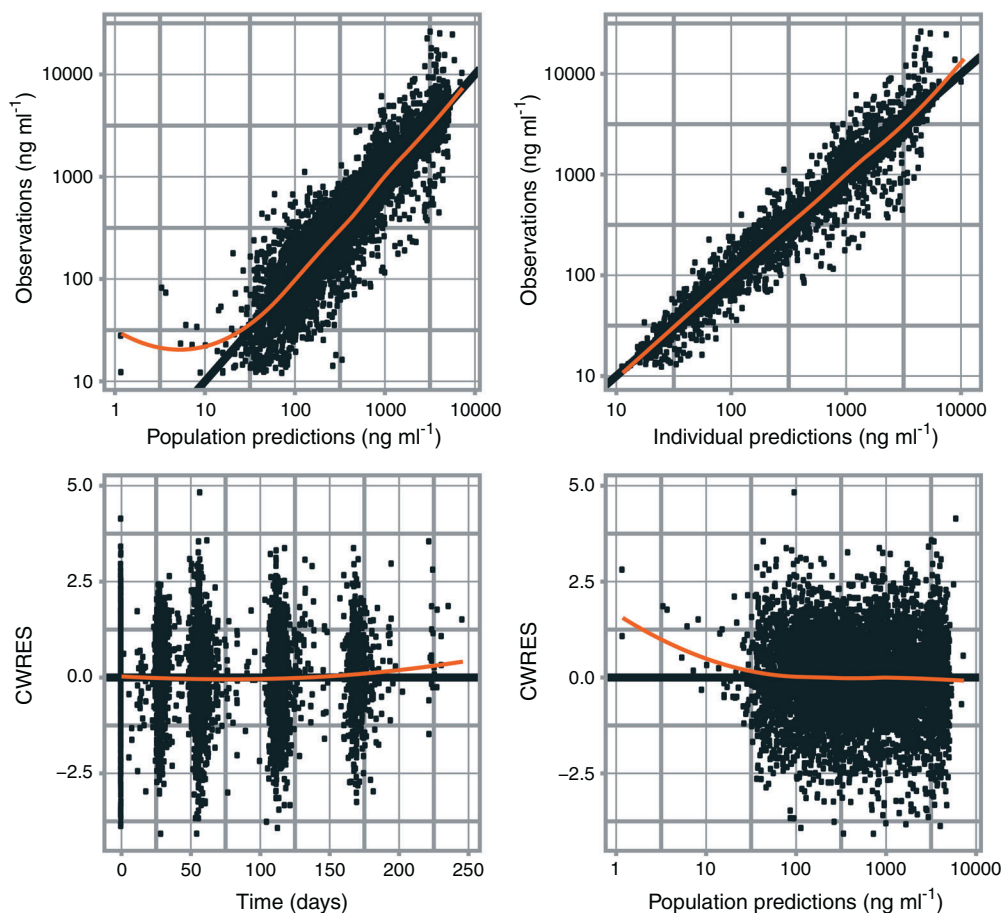


Figure 1

Goodness-of-fit plots for the final model. Black lines and points indicate individual observations. The orange lines are smoothes (loess). The solid diagonal (top row) and horizontal (lower right) black lines are the line of identity and a zero reference line, respectively. CWRES, conditional weighted residuals

related to other processes such as formation of small, multimeric (tetramers, hexamers, octamers) complexes [33]. These complexes consisting of NGF and tanezumab could result in slower clearance compared with clearance through NGF receptor internalization but faster than what is measured for antibodies not bound to target. This faster CL for tanezumab in multimeric complexes could be explained by reduced salvage by FcRn due to size-based sorting to lysosomes [34, 35]. The extent of multimeric formation would increase with increasing tanezumab concentration up to a ratio of 1 : 1 (antibody : target) and then decrease as tanezumab concentration increases [33]. Faster clearance due to complexation of therapeutic monoclonal antibody with the soluble target has been postulated for the non-linear CL of omalizumab and denosumab [36, 37].

As is typical for therapeutic antibodies, the initial volume of distribution (V_d) for tanezumab was estimated to be 2.71 l (close to plasma volume, 3 l). The volume at steady-state (V_{ss}) was approximately double the initial V_d and estimated at 4.69 l (V_1 plus V_2). This low V_d indicates that distribution of tanezumab was limited to the

interstitial space fluid. The extent of this distribution, which probably occurs primarily via convection and transcytosis [35, 38], is similar to what has been reported for other therapeutic antibodies [23].

IIV for CL and volume was moderate (20%–26%) and was as expected considering linear elimination by non-specific, high capacity endocytosis, the limited space distribution for tanezumab with no off-target binding, and with the fact that NGF is not a membrane-bound target. IIV for VM was relatively high at 41% and no covariates were identified that contributed to this variability. Because non-linear CL is most likely mediated via target binding, VM is related to the number of NGF molecules and KM would mostly reflect both the affinity of tanezumab for NGF as well as the affinity of the tanezumab–NGF complex for FcRn.

Covariates were identified that explained some IIV in CL (35%), V_1 (27%) and V_2 (20%) between patients. WT was the most significant covariate (CL, V_1 and V_2), followed by gender (CL and V_1), CL_{cr} (CL) and dose (CL). Similar covariate effects have been identified for other monoclonal antibodies [23]. The most commonly

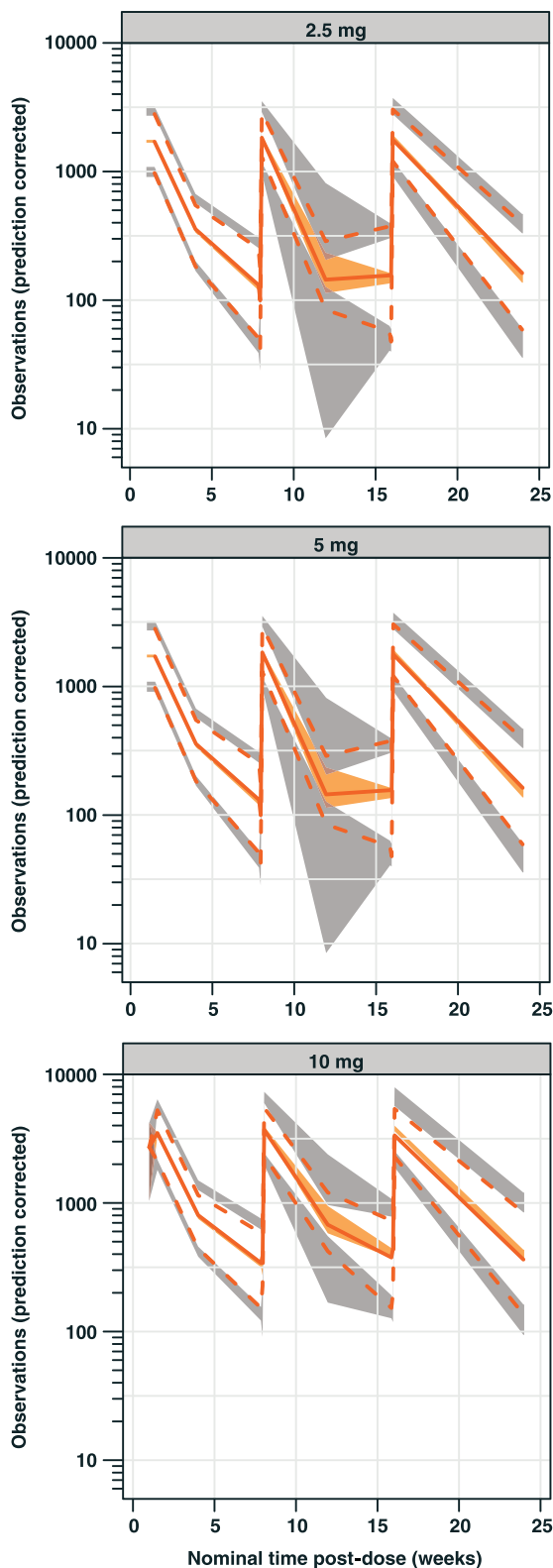


Figure 2

A prediction-corrected visual predictive check of the final model stratified by dose. The orange lines are the 5th, 50th (solid) and 95th percentile based on the observed data. The shaded areas are 95% confidence intervals for the 5th, 50th (orange) and 95th percentile. Only a small subset of individuals had observations between the second and third dose, which explains the wide simulated intervals around 12 weeks

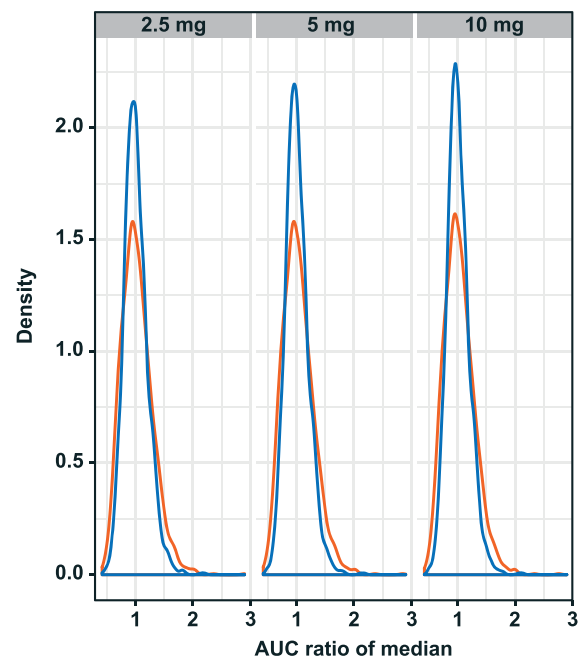




Figure 3

Histograms of ratios of the mean AUCs for fixed  and weight-adjusted  dosing regimens. AUC, area under the curve

reported covariate is body size (weight), which is associated with higher body volume as well as higher capacity to clear the drug, as is typical for both therapeutic antibodies and small molecules. Also, a higher CL and higher V_d are frequently reported in males compared with females [23, 39]. The slower clearance and lower V_d in females compared with males may be due to higher expression of the FcRn receptor in females. This is possibly caused by differences in inflammatory cytokines and/or hormonal expression that are known to modulate FcRn expression [40]. Alternatively, expression of FcRn could be lower in males due to higher muscle mass, where FcRn expression is relatively low [41].

It is less common that a statistically significant effect of CL_{cr} on total body clearance is identified, since renal clearance is not considered important for elimination of monoclonal antibodies due to their large size and inefficient filtration through the glomerulus [38], although expression of FcRn in proximal renal cells suggests possible transfer of IgG in urine by transcytosis [42]. The minor role of the kidney in IgG clearance is confirmed by population analysis results for tanezumab because the percent change in total clearance with changing CL_{cr} (Table 3) agrees with renal clearance of endogenous IgG and represents <15% of total clearance [43]. Similar CL_{cr} effects on total clearance have been reported for ustekinumab and orantuzimab [44, 45].

In this dataset, a 7% lower CL at the highest dose of 10 mg was identified compared with doses of 5 mg and 2.5 mg, independent of concentration-dependent

Table 3

The impact of the covariates on the corresponding parameter

Relation	Impact
WT on CL	10% change in WT leads to 8% change in CL
CL _{cr} on CL	10% change in CL _{cr} leads to 1% change in CL
Gender on CL	Males have 14% higher CL than females
Dose on CL	CL is 7% higher with 2.5 and 5 mg compared with 10 mg dose
WT on V ₁	10% change in WT leads to 5% change in V ₁
Gender on V ₁	Males have 18% higher V ₁ than females
WT on V ₂	10% change in body weight leads to 3% change in V ₂

CL, clearance; CL_{cr}, creatinine clearance; V₁, central volume; V₂, peripheral volume; WT, body weight.

non-linear CL. Lower CL associated with higher doses that could not be described by saturable non-linear kinetics has been observed for other antibodies as well, such as efalizumab and ING-1 [46, 47].

All of the relationships between covariates described above were highly significant due to the large number of subjects and observations, but WT had the largest influence in reducing IIV in CL from 35% to 27% with an estimated coefficient of 0.77. In contrast, the addition of all other significant covariates only reduced IIV by another 1% (from 27% to 26%). Only a small increase in variability for fixed vs. weight-adjusted dosing would be expected (Figure 3). This is consistent with the predictions from the phase 2 analysis, based on PK data from weight-adjusted doses, which indicated that a fixed-dose strategy would be appropriate for phase 3 [13, 14]. It also aligns with other work exploring how body size-based dosing impacts exposure for monoclonal antibodies in general [48]. It is also likely that the difference between weight adjusted dosing and fixed dosing would be smaller in practice due to rounding and potential errors in weight and dose calculation for the weight-

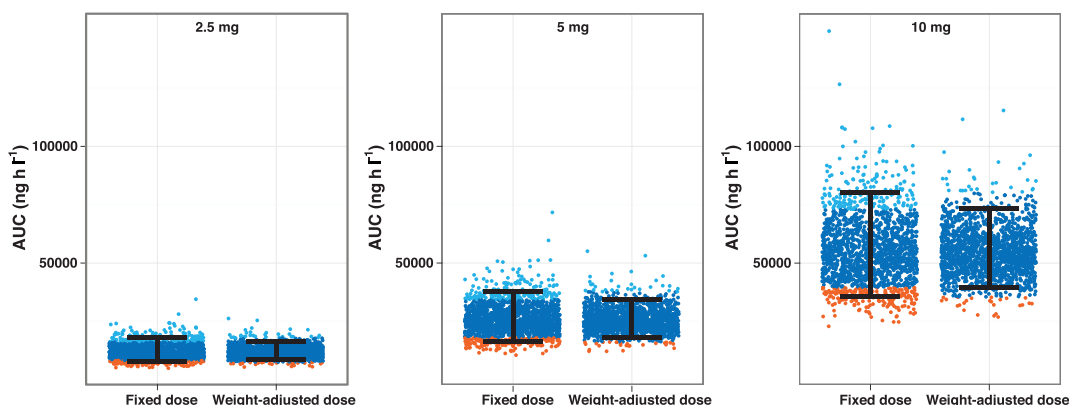
adjusted dosing. Similarly, estimated coefficients for the effect of WT on V₁ and V₂ (0.554 and 0.302, respectively) are ~0.5 or less, indicating no difference in weight-based and fixed dosing in maximum serum concentration after the initial infusion.

Across the OA programme the general safety and tolerability profile for the weight-adjusted dosing used in phase 2 [49] and fixed dosing used in phase 3 [10, 11, 48] was similar, so there was no indication that the potential small increase in variability was consequential. In particular, while there was an increased risk of rapidly progressive OA between the 5 and 10 mg doses (an adverse event most evident in the long term studies [50]), after accounting for dose, tanezumab concentration was not an additional explanatory factor (unpublished data). This finding is also consistent with the minimal overlap of predicted exposures for 5 mg and 10 mg after either weight-based or fixed dosing (Figure 4).

In conclusion, data were appropriately described by a two compartment model with a parallel linear and non-linear elimination process. The non-linear pathway was significant, but only 18% of the lowest dose was eliminated via this route. Of the covariates identified as significant, only WT had some impact on unexplained variability in CL. Still, the small increase in exposure variability for fixed vs. weight-adjusted dosing was not considered clinically relevant and supports the use of fixed dosing.

Competing Interests

All authors have completed the Unified Competing Interest form at www.icmje.org/coi_disclosure.pdf (available on request from the corresponding author) and declare ENJ was a paid consultant to carry out the data analysis with Pfizer Inc. in the previous 3 years and RX, SFM and

**Figure 4**

Comparison of the fixed and weight-adjusted dosing regimens. The points represent the predicted AUC for the individuals in the data set assuming a particular dose and dosing regimen. The black vertical bars cover 90% of the exposure ranges. The dark blue points for a given dosing regimen fall within the exposure range of the other regimen at the same dose. The light blue and orange points for one dose and regimen fall above and below the exposure range of the other regimen at the same dose, respectively. AUC, area under the curve. (● below lower limit of the fixed/adjusted dose, ● no overlap between dose levels, ● above upper limit of the fixed/adjusted dose)

RHA are employees of Pfizer Inc. This study was funded by Pfizer Inc.

Editorial support was provided by Christina McManus, PhD, of Engage Scientific Solutions and was funded by Pfizer Inc.

Contributors

E. Niclas Jonsson, Rujia Xie, Scott F. Marshall and Rosalin H. Arends wrote the manuscript, designed the research and performed the research. E. Niclas Jonsson, Scott F. Marshall and Rosalin H. Arends analyzed data.

REFERENCES

- Institute of Medicine. Relieving pain in America: a blueprint for transforming prevention, care, education, and research. Washington, DC: The National Academies Press, 2011.
- Mantyh PW, Koltzenburg M, Mendell LM, Tive L, Shelton DL. Antagonism of nerve growth factor-TrkA signaling and the relief of pain. *Anesthesiology* 2011; 115: 189–204.
- Hefti FF, Rosenthal A, Walicke PA, Wyatt S, Vergara G, Shelton DL, Davies AM. Novel class of pain drugs based on antagonism of NGF. *Trends Pharmacol Sci* 2006; 27: 85–91.
- Katz WA, Barkin RL. Dilemmas in chronic/persistent pain management. *Dis Mon* 2010; 56: 233–50.
- Woodcock J. A difficult balance—pain management, drug safety, and the FDA. *N Engl J Med* 2009; 361: 2105–7.
- Watson JJ, Allen SJ, Dawbarn D. Targeting nerve growth factor in pain: what is the therapeutic potential? *BioDrugs* 2008; 22: 349–59.
- Abdiche YN, Malashock DS, Pons J. Probing the binding mechanism and affinity of tanezumab, a recombinant humanized anti-NGF monoclonal antibody, using a repertoire of biosensors. *Protein Sci* 2008; 17: 1326–35.
- Sevcik MA, Ghilardi JR, Peters CM, Lindsay TH, Halvorson KG, Jonas BM, Kubota K, Kuskowski MA, Boustany L, Shelton DL, Mantyh PW. Anti-NGF therapy profoundly reduces bone cancer pain and the accompanying increase in markers of peripheral and central sensitization. *Pain* 2005; 115: 128–41.
- Shelton DL, Zeller J, Ho W-H, Pons J, Rosenthal A. Nerve growth factor mediates hyperalgesia and cachexia in auto-immune arthritis. *Pain* 2005; 116: 8–16.
- Brown MT, Murphy FT, Radin DM, Davignon I, Smith MD, West CR. Tanezumab reduces osteoarthritic knee pain: results of a randomized, double-blind, placebo-controlled phase III trial. *J Pain* 2012; 13: 790–8.
- Brown MT, Murphy FT, Radin DM, Davignon I, Smith MD, West CR. Tanezumab reduces osteoarthritic hip pain: Results of a randomized, double-blind, placebo-controlled phase 3 trial. *Arthritis Rheum* 2013; 65: 1795–803.
- Kivitz AJ, Gimbel JS, Bramson C, Nemeth MA, Keller DS, Brown MT, West CR, Verburg KM. Efficacy and safety of tanezumab versus naproxen in the treatment of chronic low back pain. *Pain* 2013; 154: 1009–21.
- Arends R, Lalovic B, Marshall S, Cai C-H, Olson S. Population pharmacokinetics of an anti-NGF humanized antibody, tanezumab, in patients with osteoarthritis: Support to adoption of fixed-dose regimen. Presented at American Association of Pharmaceutical Scientists – 2009, National Biotechnology Conference. 2009.
- Xie R, Arends R, Olson S, Marshall S. Preliminary pharmacokinetic/pharmacodynamic (PK/PD) analysis for the effect of tanezumab on overall daily pain score data in adults with moderate-to-severe pain due to osteoarthritis of the knee. Presented at: the 2009 annual meeting of the Population Approach Group in Europe (PAGE); 23–26 June 2009; St Petersburg, Russia. [cited 20 November 2014]. Available from http://www.page-number.org/pdf_assets/7555-PAGE%20Tanezumab%20poster%20_2009
- Ekman EF, Gimbel JS, Bello AE, Smith MD, Keller DS, Annis KM, Brown MT, West CR, Verburg KM. Efficacy and safety of intravenous tanezumab for the symptomatic treatment of osteoarthritis: two randomized controlled trials versus naproxen. *J Rheumatol* 2014; 41: 2249–59.
- U.S. Department of Health and Human Services, U.S. Food and Drug Administration, Center for Drug Evaluation and Research (CDER), Center for Biologics Evaluation and Research (CBER). Guidance for Industry: Population Pharmacokinetics. 1999 [cited 16 September 2013]. Available from [GuidanceComplianceRegulatoryInformation/Guidances/ucm072137.pdf](http://www.fda.gov/oc/ohrt/ucm072137.pdf)
- European Medicines Agency (EMA), Committee for Medicinal Products for Human Use (CHMP). Guideline on reporting the results of population pharmacokinetic analyses. 2008 [cited 16 September 2013]. Available from http://www.ema.europa.eu/docs/en_GB/document_library/Scientific_guideline/2009/09/WC500003067.pdf
- Lindbom L, Pihlgren P, Jonsson EN. PsN-Toolkit—a collection of computer intensive statistical methods for non-linear mixed effect modeling using NONMEM. *Comput Methods Programs Biomed* 2005; 79: 241–57.
- Jonsson EN, Karlsson MO. Xpose—an S-PLUS based population pharmacokinetic/pharmacodynamic model building aid for NONMEM. *Comput Methods Programs Biomed* 1999; 58: 51–64.
- Cockroft D, Gault M. Prediction of creatinine clearance from serum creatinine. *Nephron* 1976; 16: 31–41.
- Michels WM, Grootendorst DC, Verduijn M, Elliott EG, Dekker FW, Krediet RT. Performance of the Cockcroft-Gault, MDRD, and new CKD-EPI formulas in relation to GFR, age, and body size. *Clin J Am Soc Nephrol* 2010; 5: 1003–9.
- Bergstrand M, Hooker AC, Wallin JE, Karlsson MO. Prediction-corrected visual predictive checks for diagnosing nonlinear mixed-effects models. *AAPS J* 2011; 13: 143–51.

- 23 Dirks NL, Meibohm B. Population pharmacokinetics of therapeutic monoclonal antibodies. *Clin Pharmacokinet* 2010; 49: 633–59.
- 24 Zhao L, Ren TH, Wang DD. Clinical pharmacology considerations in biologics development. *Acta Pharmacol Sin* 2012; 33: 1339–47.
- 25 Mariani G, Strober W. Immunoglobulin metabolism. In: *Fc Receptors and the Action of Antibodies*, ed Metzger H. Washington, DC: American Society for Microbiology, 1990; 94–177.
- 26 Hurst SI, Arends R, Hughey DB, Vergara G, Shelton D, Liras J. Interspecies scaling of tanezumab, an anti-NGF antibody, and comparison of the projected human pharmacokinetic parameters to single-dose clinical data. Presented at Annual Scientific Meeting of the American Association of Pharmaceutical Scientists (AAPS); 2009 November 8–12; Los Angeles, CA. Available at: <http://abstracts.aaps.org/published/> (Accessed Dec 18, 2014). 2009.
- 27 Frazer JK, Capra JD. Immunoglobulins: Structure and Function. In: *Fundamental Immunology*, 4th edn, ed We P. Philadelphia: Lippincott-Raven, 1999; 37–74.
- 28 Peletier LA, Gabrielsson J. Dynamics of target-mediated drug disposition: characteristic profiles and parameter identification. *J Pharmacokinet Pharmacodyn* 2012; 39: 429–51.
- 29 Yan X, Mager DE, Krzyzanski W. Selection between Michaelis-Menten and target-mediated drug disposition pharmacokinetic models. *J Pharmacokinet Pharmacodyn* 2010; 37: 25–47.
- 30 Shooter EM. Early days of the nerve growth factor proteins. *Annu Rev Neurosci* 2001; 24: 601–29.
- 31 Nguyen CB, Harris L, Szonyi E, Baughman SA, Hale VG, Dybdal NO, Sadick MD, Escandon E. Tissue disposition and pharmacokinetics of recombinant human nerve growth factor after acute and chronic subcutaneous administration in monkeys. *Drug Metab Dispos* 2000; 28: 598–607.
- 32 Tria MA, Fusco M, Vantini G, Mariot R. Pharmacokinetics of nerve growth factor (NGF) following different routes of administration to adult rats. *Exp Neurol* 1994; 127: 178–83.
- 33 Fox JA, Hotaling TE, Struble C, Ruppel J, Bates DJ, Schoenhoff MB. Tissue distribution and complex formation with IgE of an anti-IgE antibody after intravenous administration in cynomolgus monkeys. *J Pharmacol Exp Ther* 1996; 279: 1000–8.
- 34 Busse W, Corren J, Lanier BQ, McAlary M, Fowler-Taylor A, Cioppa GD, van As A, Gupta N. Omalizumab, anti-IgE recombinant humanized monoclonal antibody, for the treatment of severe allergic asthma. *J Allergy Clin Immunol* 2001; 108: 184–90.
- 35 Wefflen AW, Baier N, Tang QJ, Van den Hof M, Blumberg RS, Lencer WI, Massol RH. Multivalent immune complexes divert FcRn to lysosomes by exclusion from recycling sorting tubules. *Mol Biol Cell* 2013; 24: 2398–405.
- 36 Gibiansky L, Sutjandra L, Doshi S, Zheng J, Sohn W, Peterson MC, Jang GR, Chow AT, Perez-Ruixo JJ. Population pharmacokinetic analysis of denosumab in patients with bone metastases from solid tumours. *Clin Pharmacokinet* 2012; 51: 247–60.
- 37 Hayashi N, Tsukamoto Y, Sallas WM, Lowe PJ. A mechanism-based binding model for the population pharmacokinetics and pharmacodynamics of omalizumab. *Br J Clin Pharmacol* 2007; 63: 548–61.
- 38 Lobo ED, Hansen RJ, Balthasar JP. Antibody pharmacokinetics and pharmacodynamics. *J Pharm Sci* 2004; 93: 2645–68.
- 39 Fasanmade AA, Adedokun OJ, Ford J, Hernandez D, Johanns J, Hu C, Davis HM, Zhou H. Population pharmacokinetic analysis of infliximab in patients with ulcerative colitis. *Eur J Clin Pharmacol* 2009; 65: 1211–28.
- 40 Dostalek M, Gardner I, Gurbaxani BM, Rose RH, Chetty M. Pharmacokinetics, pharmacodynamics and physiologically-based pharmacokinetic modelling of monoclonal antibodies. *Clin Pharmacokinet* 2013; 52: 83–124.
- 41 Chen Y, Balthasar JP. Evaluation of a catenary PBPK model for predicting the *in vivo* disposition of mAbs engineered for high-affinity binding to FcRn. *AAPS J* 2012; 14: 850–9.
- 42 Akilesh S, Huber TB, Wu H, Wang G, Hartleben B, Kopp JB, Miner JH, Roopenian DC, Unanue ER, Shaw AS. Podocytes use FcRn to clear IgG from the glomerular basement membrane. *Proc Natl Acad Sci USA* 2008; 105: 967–72.
- 43 Waldmann TA, Strober W. Metabolism of immunoglobulins. *Prog Allergy* 1969; 13: 1–110.
- 44 Xin Y, Jin D, Eppler S, Damico-Beyer LA, Joshi A, Davis JD, Kaur S, Nijem I, Bothos J, Peterson A, Patel P, Bai S. Population pharmacokinetic analysis from phase I and phase II studies of the humanized monovalent antibody, onartuzumab (MetMab), in patients with advanced solid tumors. *J Clin Pharmacol* 2013; 53: 1103–11.
- 45 Zhu Y, Hu C, Lu M, Liao S, Marini JC, Yohrling J, Yeilding N, Davis HM, Zhou H. Population pharmacokinetic modeling of ustekinumab, a human monoclonal antibody targeting IL-12/23p40, in patients with moderate to severe plaque psoriasis. *J Clin Pharmacol* 2009; 49: 162–75.
- 46 de Bono JS, Tolcher AW, Forero A, Vanhove GF, Takimoto C, Bauer RJ, Hammond LA, Patnaik A, White ML, Shen S, Khazaeli MB, Rowinsky EK, LoBuglio AF. ING-1, a monoclonal antibody targeting Ep-CAM in patients with advanced adenocarcinomas. *Clin Cancer Res* 2004; 10: 7555–65.
- 47 Sun YN, Lu JF, Joshi A, Compton P, Kwon P, Bruno RA. Population pharmacokinetics of efalizumab (humanized monoclonal anti-CD11a antibody) following long-term subcutaneous weekly dosing in psoriasis subjects. *J Clin Pharmacol* 2005; 45: 468–76.
- 48 Wang DD, Zhang S, Zhao H, Men AY, Parivar K. Fixed dosing versus body size-based dosing of monoclonal antibodies in adult clinical trials. *J Clin Pharmacol* 2009; 49: 1012–24.
- 49 Lane NE, Schnitzer TJ, Birbara CA, Mokhtarani M, Shelton DL, Smith MD, Brown MT. Tanezumab for the treatment of pain from osteoarthritis of the knee. *N Engl J Med* 2010; 363: 1521–31.
- 50 Pfizer Inc. Tanezumab Arthritis Advisory Committee Briefing Document. 2012 [cited 1 June 2015]. Available from <http://www.fda.gov/downloads/AdvisoryCommittees/CommitteesMeetingMaterials/Drugs/ArthritisDrugsAdvisoryCommittee/UCM295205.pdf>

Supporting Information

Additional Supporting Information may be found in the online version of this article at the publisher's web-site:

In brief, microtitre assay plates were coated with recombinant human NGF overnight, then washed (wash buffer: 1× phosphate buffered saline [PBS]/0.3 M NaCl/0.05% polysorbate-20 or PBS-T/0.3 M NaCl, pH 7.4) to block unadsorbed sites with blocking buffer. Calibration standards (6.0–384 ng ml⁻¹) and quality control (QC) samples were prepared by diluting the tanezumab reference standard into human serum with diluent buffer 1 : 20. Following incubation (covered and incubated at ambient

temperature for at least 60 min with non-vigorous shaking), plates were washed with blocking buffer, and polyclonal donkey anti-human IgG conjugated with horseradish peroxidase was added for binding to captured tanezumab. After the final wash, a chemiluminescent substrate solution (working substrate solution: Supersignal ELISA Femto Maximum Sensitivity Chemiluminescent Substrate System) was added. After 8 to 9 min incubation, relative light units of luminescence (which develops proportionally to the amount of tanezumab) were measured on a luminescence plate reader (Bio-Tek Clarity; Clarity 4.0 Rev. 2 or higher, Winooski, VT, USA).